Published in final edited form as:
Basic Res Cardiol. 2011 September ; 106(5): 849–864. doi:10.1007/s00395-011-0180-1.

Intracoronary administration of cardiac stem cells in mice: a new, improved technique for cell therapy in murine models

Qianhong Li, **Yiru Guo**, **Qinghui Ou**, **Ning Chen**, **Wen-Jian Wu**, **Fangping Yuan**, **Erin O'Brien**, **Tao Wang**, **Li Luo**, **Gregory N. Hunt**, **Xiaoping Zhu**, and **Roberto Bolli**
Division of Cardiovascular Medicine, University of Louisville, 550 S. Jackson Street, Louisville, KY 40292, USA

Roberto Bolli: rbolli@louisville.edu

Abstract

A model of intracoronary stem cell delivery that enables transgenesis/gene targeting would be a powerful tool but is still lacking. To address this gap, we compared intracoronary and intramyocardial delivery of $lin^-/c\text{-}kit^+/GFP^+$ cardiac stem cells (CSCs) in a murine model of reperfused myocardial infarction (MI). $Lin^-/c\text{-}kit^+/GFP^+$ CSCs were successfully expanded from GFP transgenic hearts and cultured with no detectable phenotypic change for up to ten passages. Intracoronary delivery of CSCs 2 days post-MI resulted in significant alleviation of adverse LV remodeling and dysfunction, which was at least equivalent, if not superior, to that achieved with intramyocardial delivery. Compared with intramyocardial injection, intracoronary infusion was associated with a more homogeneous distribution of CSCs in the infarcted region and a greater increase in viable tissue in this region, suggesting greater formation of new cardiomyocytes. Intracoronary CSC delivery resulted in improved function in the infarcted region, as well as in improved global LV systolic and diastolic function, and in decreased LV dilation and LV expansion index; the magnitude of these effects was similar to that observed after intramyocardial injection. We conclude that, in the murine model of reperfused MI, intracoronary CSC infusion is at least as effective as intramyocardial injection in limiting LV remodeling and improving both regional and global LV function. The intracoronary route appears to be superior in terms of uniformity of cell distribution, myocyte regeneration, and amount of viable tissue in the risk region. To our knowledge, this is the first study to report that intracoronary infusion of stem cells in mice is feasible and effective.

Keywords

Intracoronary administration; Cardiac stem cells; Regeneration; Mice; Myocardial infarction; Cardiac function

Introduction

Transplantation of stem cells is emerging as a potentially transformative strategy to ameliorate left ventricular (LV) remodeling and dysfunction after acute myocardial infarction (MI) [7, 11-13, 20, 36]. Among the many types of cells being investigated, $c\text{-}kit^+$ cardiac stem cells (CSCs) appear to be particularly promising because they normally reside in the adult myocardium, are responsible for the physiologic turnover of cardiac cells, and

Correspondence to: Roberto Bolli, rbolli@louisville.edu.

Q. Li and Y. Guo contributed equally to this study.

have repeatedly been shown to be capable of differentiating into all three major cardiac cell types (myocytes, smooth muscle cells, and endothelial cells) in vitro and to improve LV remodeling and dysfunction after both a recent and an old MI in various animal models [15, 38]. Importantly, the first-in-human study of c-kit$^+$ CSCs (SCIPIO, Stem Cell Infusion in Patients with Ischemic Cardiomyopathy, http://www.clinicaltrials.gov/ct2/show/NCT00474461) is ongoing, with initial results that are encouraging [6].

For administration of CSCs to become a widespread therapeutic approach to the treatment of acute MI and heart failure, it will be necessary to utilize a delivery modality that is readily applicable to most clinical settings. The preponderance of preclinical studies has injected CSCs directly into the myocardium with a needle, but this approach has two important limitations. First, the cells are delivered only to relatively small myocardial areas, resulting in nonuniform distribution within the recipient heart, which may limit their ability to affect global LV function. Second, intramyocardial injection of CSCs would be difficult to achieve clinically on a widespread basis, for it would necessitate the purchase of expensive equipment and the availability of specialized expertise, both of which may not be feasible in the majority of hospitals. For this reason, almost all clinical trials of stem cells have used the intracoronary infusion route [1]. Intracoronary infusion has been shown to be effective in promoting homing, engraftment, and differentiation of various stem cells and in producing substantial functional and structural benefits in preclinical models as well as in patients [1, 12]. In view of this track record of proven efficacy, and in view of its practicality, the intracoronary route appears to be the most suitable for widespread clinical applications of CSC therapy.

These considerations emphasize the importance of preclinical models of intracoronary CSC delivery. While intracoronary infusion of CSCs has been shown to be effective in rats [38] and pigs [25], its efficacy in murine models of MI and heart failure is unknown. Compared with the rat and pig models, the murine model offers the important advantage of enabling investigators to manipulate gene expression via transgenesis and knockout, thereby establishing unequivocally a functional role of a specific protein in stem cell activity and its resulting therapeutic effects. Analogous genetic manipulations would be impossible, impractical, and/or inordinately expensive in larger species such as rats and pigs. Consequently, it is of the utmost importance to determine whether the intracoronary route of CSC administration is feasible in mice and, if so, whether this treatment produces salubrious effects, similar to those observed in other species.

The goal of this study was to develop a method for delivering CSCs intracoronarily in mice and to compare the effects of this therapy with those of the traditional intramyocardial delivery approach. Using a murine model of reperfused MI, we report here that intracoronary infusion of CSCs is feasible and is associated with the mortality comparable to that associated with intramyocardial delivery. We further demonstrate that intracoronary delivery results in effective transplantation of CSCs and imparts beneficial effects that are at least equivalent, and possibly superior, to those achieved by the traditional intramyocardial injection. This murine model of cell therapy should be useful to conduct mechanistic investigations of CSCs in a clinically relevant setting.

Methods

This study was performed in accordance with the *Guide for the Care and Use of Laboratory Animals* (Department of Health and Human Services, Publication No. [NIH] 86–23) and with the guidelines of the Animal Care and Use Committee of the University of Louisville, School of Medicine (Louisville, KY, USA).

Mouse lin$^-$/c-kit$^+$/GFP$^+$ CSC isolation and culture

Lin$^-$/c-kit$^+$/GFP$^+$ CSCs were isolated from GFP transgenic mice expressing GFP under the control of the human ubiquitin C promoter (C57BL6 background, 8–10 weeks of age). Hearts were finely minced and cultured to establish cell outgrowth cultures over ~7 days using growth medium (F12 K medium supplemented with bFGF, LIF, and 10% FBS) [4, 9]. Lin$^-$/c-kit$^+$ CSCs were isolated from the cell outgrowth of the explants by sequential sorting. First, outgrowth cells were depleted of mature hematopoietic lin$^+$ cells, including T cells, B cells, thymocytes, monocytes/macrophages, granulocytes, neutrophils, erythrocytes, and their committed bone marrow precursors. For this purpose, cells were labeled using magnetic microbeads conjugated to a cocktail of antibodies against a panel of lineage antigens including CD5 (T and B lymphocytes and thymocytes), CD45R (B lymphocytes), CD11b (macrophages), GR-1 (granulocytes), 7-4 (neutrophils), and TER-119 (erythrocytes) (Miltenyi Biotec Inc., CA, USA). This labeling procedure allows isolation of lineage negative cells lacking the markers of interest. The lin$^-$ cells were then sorted for c-kit with a specific anti-c-kit antibody (Santa Cruz) and magnetic immunobeads (Miltenyi). To maximize results, the c-kit sorting procedure was repeated three consecutive times at 14-day intervals. The lin$^-$/c-kit$^+$ cells were cultured, and the purity of the sorted cells was confirmed quantitatively by flow cytometry and immunofluorescent staining before use [4, 9]. In all studies, the lin$^-$/c-kit$^+$/GFP$^+$ CSCs used for cell transplantation in vivo were passaged 4–6 times; those used for stem cell biology analyses in vitro were passaged less than ten times.

Flow cytometric analysis

To verify the purity of the c-kit positive cells in the sorted GFP$^+$ cell population, CSC suspensions (1×10^6 cells per aliquot) were labeled with specific anti-c-kit and anti-GFP antibodies (Santa Cruz). To detect the transcription factors expressed early in cardiovascular specification, aliquots of 1×10^6 CSCs were labeled with specific anti-Ets-1, anti-GATA-6, anti-GATA-4, anti-MEF2C, and anti-Nkx2.5 antibodies (Santa Cruz) [4, 9]. Samples were analyzed by flow cytometry (BD LSRII, Becton–Dickinson), and 20,000–50,000 events were collected per sample ($n = 3$).

Migration assay

Migration of murine CSCs was assayed in a Boyden chamber with 8-μm pore polycarbonate filters (Cell Bio-labs, San Diego, CA, USA). The lower chamber was filled with 500 μl of serum-free medium containing various concentrations of SDF-1α (Sigma). CSCs were then suspended at a concentration of 3×10^3 cells in 300 μl of serum-free medium and added to the upper chamber. The upper and lower chambers were separated by 8-μm pore polycarbonate filters. The chamber was incubated for 16 h at 37°C in a humid atmosphere of 5% CO_2. After incubation, the migrated cells were dissociated from the membrane by addition of cell detachment buffer to the lower chamber, then lysed and quantified using CyQuant GR Fluorescent Dye for fluorescence measurement with a fluorescence plate reader at 480 nm/520 nm [34].

Western immunoblotting analysis

Protein samples were isolated from CSCs as previously described [27, 28]. The expression of c-kit in the membranous fraction and of GFP in the cytosolic fraction was assessed by standard SDS/PAGE Western immunoblotting with specific anti-c-kit and anti-GFP antibodies (Santa Cruz) [28, 30].

Murine model of postinfarction LV remodeling and failure

The study was performed in C57BL6/J female mice, 20.2 ± 0.4 g (age 11–12 weeks), purchased from The Jackson Laboratory (Bar Harbor, ME, USA). All mice were maintained

in microisolator cages under specific pathogen-free conditions in a room with a temperature of 24°C, 55–65% relative humidity, and a 12-h light–dark cycle. The murine model of myocardial ischemia and reperfusion has been described in detail [19, 27, 28]. Briefly, mice were anesthetized with sodium pentobarbital (60 mg/kg i.p.) and ventilated using carefully selected parameters. The chest was opened through a midline sternotomy, and a nontraumatic balloon occluder was implanted around the mid-left anterior descending coronary artery using an 8-0 nylon suture. To prevent hypotension, blood from a donor mouse was given at serial times during surgery. Rectal temperature was carefully monitored and maintained between 36.7 and 37.3°C throughout the experiment. In all groups, MI was produced by a 60-min coronary occlusion followed by reperfusion (Fig. 1). Successful performance of coronary occlusion and reperfusion was verified by visual inspection (i.e., by noting the development of a pale color in the distal myocardium after inflation of the balloon and the return of a bright red color due to hyperemia after deflation) and by observing S-T segment elevation and widening of the QRS on the ECG during ischemia and their resolution after reperfusion). Mice were then followed for 41 days. Beginning at the time of cell transplantation and continuing until euthanasia (for 39 days), BrdU (Sigma) was infused (33 mg/kg/day) with Alzet® mini-osmotic pumps (Durect Corp., CA, USA) to identify newly formed cells [32].

CSC transplantation

Intracoronary cell delivery—Forty-eight hours after reperfusion, mice were randomly allocated to a control or a cell-treated group. They were reanesthetized, the chest was reopened through a central thoracotomy, and the aortic root was exposed by blunt dissection. A 30-gauge needle connected to a 100-μl syringe was advanced to the aortic root through the LV apex. The proximal aorta and pulmonary artery were cross-clamped with a snare for 10 s, during which time mice received an intracoronary infusion of CSCs (4×10^5 cells in 80 μl of PBS) or vehicle. After a clamp time of 10 s, aortic flow was restored.

Intramyocardial cell delivery—The technique for CSC transplantation by intramyocardial injection was similar to that used in our previous studies of gene and cell transfer [16, 27, 28, 30]. Briefly, at 48 h after MI, mice were reanesthetized and the chest reopened through a central thoracotomy. $Lin^-/c\text{-}kit^+/GFP^+$ CSCs (10^5 cells in 40 μl) or an equivalent volume of vehicle were injected intramyocardially using a 30-gauge needle. A total of four injections (10 μl each) were made in the peri-infarct region in a circular pattern, at the border between infarcted and noninfarcted myocardium. The number of cells injected (10^5) was the maximal number that can be delivered via this route; injection of higher CSC numbers would not be feasible in the small mouse heart.

Echocardiographic studies

Serial echocardiograms were obtained at baseline (4 days prior to the coronary occlusion/reperfusion), 2 days after CSC treatment (4 days after MI), and 35 days after CSC transplantation (4 days prior to hemodynamic studies and euthanasia) (Fig. 1) using a Vevo 2100 high frequency, high resolution (30 micron) digital imaging ultrasound system (VisualSonics, Inc.) equipped with 24 and 38 MHz Microscan transducers and linear array technology for B-mode and M-mode imaging and color Doppler mode scanning. We have performed careful studies comparing three anesthetic agents (i.p. pentobarbital, i.p. ketamine/xylazine, and inhaled isoflurane); of these, isoflurane caused the least perturbations in heart rate and cardiac function [14, 29]. Thus, all of the echocardiographic studies were performed under isoflurane anesthesia. Using a rectal temperature probe, body temperature was carefully maintained between 36.7 and 37.3°C throughout the study. Digital images were analyzed off-line by blinded observers using the Vevo 2100 workstation software. At least three measurements were taken and averaged for each

parameter. Standard echocardiographic parameters were derived from the two-dimensional, M-mode, and Doppler images, as in our previous studies [14, 29].

Hemodynamic studies

Hemodynamic studies were performed just before euthanasia (Fig. 1) using the ARIA-1 system consisting of MPCU-200 P–V signal conditioning hardware, 1.0 French PVR-1035 microtip ultra-miniature pressure–volume (PV) catheters (Millar Instruments), data acquisition software, and PVAN data analysis software. Mice were anesthetized with isoflurane and rectal temperature kept between 36.7 and 37.3°C. A 1.0 French Millar catheter was inserted into the LV via the right carotid artery [17, 18, 42]. Inferior vena cava occlusion was performed with external compression to produce variably loaded beats for determination of the end-systolic PV relation (ESPVR) and other derived constructs of LV performance. The raw pressure and volume data collected in text files by the MPCU-200 unit and Chart/Powerlab software were imported into the PVAN software, which applied a variety of algorithms to the P–V data to calculate up to 30 cardiovascular parameters [5, 37]. As in the case of the echo studies, all hemodynamic data analyses were performed off-line by investigators blinded to the treatment.

Heart fixation and morphometric analysis

At the conclusion of the protocol, the heart was arrested in diastole by an i.v. injection of 0.15 ml of $CdCl_2$ (100 mM), excised, and perfused retrogradely at 60–80 mmHg (LVEDP = 8 mmHg) with heparinized PBS followed by 10% neutral buffered formalin solution for 15 min. The heart was then sectioned into three slices from apex to base, fixed in formalin for 24 h, and subjected to tissue processing and paraffin embedding. Paraffin-embedded LV blocks were sectioned at a thickness of 4 μm for histochemistry and immunohistochemistry [4, 9, 38, 41]. Morphometric parameters, including LV cavity area, total LV area, risk region area, scar area, LV wall thickness, and infarct expansion index were measured in sections stained with Masson's trichrome as described in our previous studies [38]. Images were analyzed using NIH Image J (1.42v) and measurements from the various slices averaged [38, 41].

Immunohistochemistry

Formalin-fixed, paraffin-embedded, 4 μm-thick heart sections were deparaffinized in xylene and rehydrated gradually through 100, 95, and 70% ethanol followed by antigen retrieval procedure. After pre-incubation with serum blocking solution, persistence of transplanted $lin^-/c\text{-}kit^+/GFP^+$ CSCs (or their progeny) was determined by GFP immunofluorescent staining and confocal microscopy. The fate of transplanted CSCs was assessed by double staining with specific monoclonal antibodies against GFP (Santa Cruz) and against cardiac-specific marker (α-sarcomeric actin) (Sigma). CSC proliferation was assessed by immunofluorescent staining of nuclei for BrdU [32], using a mouse monoclonal antibody (Santa Cruz). In all of the immunofluorescent staining procedures, secondary antibodies conjugated with the appropriate fluorochrome (Jackson ImmunoResearch) were used. The concentration of primary and secondary antibodies corresponded to that indicated by the manufacturer. To minimize autofluorescence, slides were incubated with 0.1% Sudan Black B (Sigma), rinsed in PBS, and then mounted with ProLong Gold antifade reagent (Invitrogen). Immunohistochemical signals were imaged by confocal microscopy and quantitatively analyzed by Image J (1.42q, NIH). In each heart, GFP^+ cells, GFP^+/α-sarcomeric $actin^+$ (double positive) cells, and total nuclei were counted in 25 confocal images acquired from the infarcted area (ten images), each of the two border zones (five images per border zone), and non-infarcted area (five images), totaling 0.51 mm^2 per heart. For $BrdU^+$ cell counting, approximately 15, 000 nuclei per heart were counted in 25 confocal images as described above. In all cases, at least four hearts per group were

examined. CSC immunocytochemistry was performed with cell-smeared slides fixed in 4% paraformaldehyde. CSC immunofluorescent staining was performed with specific antibodies against GFP, c-kit, Nkx-2.5, MEF2C (Santa Cruz), and α-sarcomeric actin (Sigma) [4, 9, 32, 41].

Statistical analysis

Data are presented as mean ± SEM. All data were analyzed with one-way analysis of variance (ANOVA for normally distributed data, or Kruskal–Wallis one way analysis of variance on ranks for data that are not normally distributed), as appropriate, followed by unpaired Student's *t* tests with the Bonferroni correction. A P value <0.05 was considered statistically significant. All statistical analyses were performed using the SigmaStat software system (3.5 V) [8, 27, 43].

Results

Exclusions

A total of 91 mice were used for this study. Thirty-nine mice died during or shortly after the surgical procedure: 20 after the first surgery (coronary occlusion) and 19 after the second surgery (cell transplantation; seven died in the vehicle group and 12 in the CSC group). Three mice (3.3%) were excluded because of technical problems, including body temperature out of normal range ($n = 1$), balloon occluder malfunction ($n = 1$), and bleeding during the surgery ($n = 1$). Thus, a total of 49 mice were included in the final analyses.

Fundamental physiological parameters

During the echocardiographic and hemodynamic studies, heart rate and body temperature (fundamental physiological parameters that may impact myocardial function) were similar in vehicle and treated groups within the same delivery route (i.m. or i.c.) (Table 1). By experimental design, rectal temperature remained within a narrow, physiologic range (36.8–37.2°C) in all groups.

Isolation, sorting, and characterization of murine CSCs

As indicated above, minced mouse hearts were cultured by the primary explant technique. Successful cell outgrowth was obtained in all hearts ($n = 12$). A monolayer of ~5×10^3 cells was present at the periphery of each tissue aggregate at 7 days after primary culture (Fig. 2a, b). Using a cocktail of biotin-conjugated-specific antibodies against lineage antigens including CD5, CD45R, CD11b, GR-1, 7-4, and TER-119, lineage-positive cells were depleted with antibody-labeled magnetic microbeads (Miltenyi); 61.3 ± 5.8% of the unfractionated population was lin^- ($n = 22$) and 38.7 ± 2.4% was lin^+. Lin^- cells were further sorted with immunobeads against c-kit to obtain an enriched population of $lin^-/c\text{-}kit^+$ CSCs. $Lin^-/c\text{-}kit^+$ CSCs constituted 7.8 ± 0.9% of the lin^- cell population; this was confirmed by both flow cytometric analysis and immunofluorescent staining (Fig. 2). To maximize results, the c-kit sorting procedure was repeated three consecutive times at 14-day intervals. During culture, c-kit expression (determined by flow cytometric analysis) remained >95% from passage 2 to passage 10, averaging 97.3 ± 2.0% at passage 2, 98.0 ± 1.9% at passage 4, 96.5 ± 1.2% at passage 6, 97.7 ± 1.1% at passage 8, and 97.6 ± 2.5% at passage 10 (Fig. 2d). The results of Western blot analyses were consistent with uniformly high levels of c-kit expression (Fig. 2e). Thus, this protocol (three c-kit sorting procedures) results in a highly enriched cell population that reproducibly consists of >95% $lin^-/c\text{-}kit^+$ CSCs and maintains very high (>95%) and stable c-kit expression for up to ten passages. Furthermore, Western immunoblotting and flow cytometric analyses indicated that GFP expression in the sorted $lin^-/c\text{-}kit^+/GFP^+$ CSCs was very high (>99%) and uniform (Fig. 2f,

g). The expression of c-kit in the membrane and of GFP in the cytoplasm was further confirmed by immunofluorescent staining of the smears of purified GFP^+ CSCs (Fig. 2h). The average diameter of the $lin^-/c\text{-}kit^+$ CSCs was 8.08 ± 0.16 μm [n = 96; measured by Image J (1.42q, NIH)].

As illustrated in Fig. 3, when CSCs were cultured in growth medium (cells labeled as "undifferentiated" in Fig. 3), a subset expressed the cardiac transcription factors Nkx-2.5 (Fig. 3a–c) and MEF2 (Fig. 3d–f). This was confirmed by flow cytometric analysis (17.0 ± 2.2 and 15.8 ± 2.3%, n = 5, respectively) and further demonstrated by a 3-D computer reconstruction of a representative CSC acquired from 42 confocal microscopic images, showing c-kit (red) on the membrane and the early cardiac transcription factor MEF2C (green) in the nucleus (blue) (Fig. 3j). Subsets of $lin^-/c\text{-}kit^+$ CSCs also expressed GATA-4 (5.0 ± 1.3%), GATA-6 (4.9 ± 1.0%), and Ets-1 (14.6 ± 2.1%) (n = 5, Fig. 3). Expression of Nkx-2.5, MEF2, and GATA4 demonstrates the potential of CSCs to commit to the myogenic lineage, while expression of GATA-6 and Ets-1 indicates potential to commit to the vascular smooth muscle and endothelial lineages, respectively.

To test the differentiation characteristics of CSCs, sub-confluent CSCs at passage 6 were cultured in differentiation medium (10^{-8} M dexamethasone without LIF) [4] (cells labeled as "differentiated" in Fig. 3). Ten days later, flow cytometric analysis showed increased expression of the lineage markers Ets-1 (endothelial), GATA-6 (smooth muscle), and GATA-4, MEF2C, and Nkx-2.5 (myocytic), confirming that $lin^-/c\text{-}kit^+$ CSCs have the potential to commit to all three cardiac lineages (Fig. 3). Consistent with the flow cytometric results, immunofluorescent staining demonstrated that cells cultured in differentiation medium in Matrigel started to express α-sarcomeric actin in the cytoplasm after 10 days (Fig. 3g, h) and a cardiac myocyte-like morphology in the culture plate without Matrigel after 50 days (Fig. 3i).

The doubling time of CSCs in culture was analyzed by flow cytometry (CellTrace Violet, Invitrogen) at multiple time points over a 4-day period. No significant changes were observed during ten passages with regard to the time required for population doubling (45.5 ± 0.8 h, n = 4). The migration properties of CSCs were assayed in a Boyden chamber with 8-μm pore polycarbonate filters (Cell Biolabs). Serum-free medium containing various concentrations of SDF-1α was added into the lower wells of the Boyden chamber, and CSCs were loaded into the upper inserts. With increasing concentrations of SDF-1α (50–200 ng/ml), a dose-dependent increase in migration of CSCs was observed after 16 h, indicating that the isolated $lin^-/c\text{-}kit^+$ cells exhibit a functional migratory response to SDF-1α stimulation (Fig. 4).

CSC distribution in the heart after transplantation

Intracoronary delivery was achieved by infusing CSCs in the left ventricle as the aorta and pulmonary artery were cross-clamped distal to the needle tip for 10 s. During this period, the right and left ventricles became visibly pale, as the clear cell solution perfused the myocardium through the coronary arteries; heart rate decreased from 564 ± 13 to 314 ± 12 bpm (n = 17), but recovered to baseline within 1.19 ± 0.14 min of clamp release (n = 17).

Figure 5a–d illustrates the pattern observed 2 days following CSC delivery (i.e., 4 days after a 60-min coronary occlusion) when the cells were delivered via the intramyocardial route (i.e., when they were directly injected with a needle in the border zones of the infarcted region). The distribution of CSCs was inhomogeneous and focal, i.e., they were clustered non-uniformly in the risk region with a patchy distribution and were observed only near the injection sites. Most of the infarct contained very few CSCs, and virtually no CSCs were found in the noninfarcted region (Fig. 5a–d). In contrast, 2 days following intracoronary

CSC delivery, the distribution of CSCs was relatively homogeneous (Fig. 5e–h). CSCs were uniformly distributed throughout the entire infarct (where their density was higher) and were also uniformly distributed in the noninfarcted region (where their density was lower).

Echocardiographic assessment

Before the 60-min coronary occlusion (baseline), all parameters of LV function and dimensions measured by echocardiography were similar in the four groups (Fig. 6). At 48 h after CSC transplantation (4 days after reperfusion), the degree of LV functional impairment and dilatation was also similar among the four groups (Fig. 6), indicating that the injury sustained during myocardial ischemia/reperfusion and that associated with intramyocardial injection and intracoronary infusion were comparable.

The two vehicle groups (intramyocardial and intracoronary) exhibited the expected changes in LV function and dimensions that are associated with post-MI LV failure and remodeling. Between 4 and 37 days after reperfusion, the parameters of regional myocardial function [thickening fraction (ThF) in the infarcted wall] and global LV performance [LV ejection fraction (EF)] exhibited either no change or a deterioration (Fig. 6), while there was a major decrease in wall thickness (WT) in the infarcted wall and a striking increase in LV end-diastolic volume (EDV) (Fig. 6). In contrast, in CSC-treated mice (both those that received intracoronary infusion and those that received intramyocardial injection), infarct wall ThF and LV EF increased at 37 days compared with 4 days after reperfusion; infarct WT did not decrease and the increase in EDV was much less pronounced. As a result, at 37 days, both CSC-treated groups (intracoronary and intramyocardial) exhibited significantly greater ThF in the infarcted wall (Fig. 6a), LV EF (Fig. 6b), and infarct WT (Fig. 6e) and smaller LV EDV (Fig. 6g) compared with the respective vehicle groups. The attenuation of LV dysfunction and remodeling in the intracoronary infusion group was significantly greater than that in the intramyocardial injection group, as evidenced by the fact that EF was higher (63.6 ± 1.2 vs. 54.1 ± 2.1%; $P < 0.05$; Fig. 6b) and EDV smaller (36.5 ± 1.6 vs. 41.4 ± 1.6 μl; $P < 0.05$, Fig. 6g) compared with the intramyocardial injection group.

Hemodynamic measurements

To prevent any after-effects of the anesthesia used during the echocardiographic assessment 35 days after CSC transplantation, a 4-day interval was allowed between echocardiographic and hemodynamic measurements; thus, the hemodynamic studies were performed just before euthanasia, 39 days after CSC or vehicle administration (the number of mice with hemodynamic data was less than that of mice with echocardiographic data because some animals died during the hemodynamic study). Compared with the age-matched mice not subjected to surgery (sham control group), all LV functional parameters were markedly depressed in the four groups of infarcted mice, but the deterioration was less in the two CSC-treated groups than in the respective vehicle groups (Fig. 7). This was the case not only for load-dependent (LV EF and LV dP/dt) but also for load-independent (end-systolic elastance and Tau) indices of LV systolic function (Fig. 7). Thus, the two independent methods of functional assessment (echocardiography and hemodynamic studies) consistently demonstrated that CSC administration (by the intracoronary or intramyocardial route) improved LV systolic performance.

Morphometric analysis

The effects of CSC transplantation on LV remodeling were assessed by Masson's trichrome staining. In each heart, a detailed quantitative analysis was performed on three serial LV sections taken at ~100–120-μm intervals along the LV longitudinal axis. To quantitate both the degree of LV dilation and the degree of infarct wall thinning, the LV expansion index was calculated using a modification of the method of Hochman and Choo [22]: LV

expansion index = (LV cavity area/LV total area) × (non-infarcted region wall thickness/risk region wall thickness). As illustrated in Fig. 8, morphometric analysis demonstrated that there were no appreciable differences among the four groups with respect to the size of the region at risk (expressed as a percentage of the left ventricle), indicating that the magnitude of the ischemic insult was comparable in all groups. Both CSC delivery routes resulted in an increase in the amount of viable myocardium in the region at risk, concomitant with an increase in LV anterior wall (infarct wall) thickness and a reduction in the LV expansion index (Fig. 8). The increased amount of viable myocardium translates into a reduction in scar area: in mice that received intracoronary CSCs, the scar area (21.3 ± 1.4% of the region at risk) was not only smaller than that in the corresponding vehicle-treated group (32.4 ± 2.5%; $P < 0.01$) but also smaller than that in mice treated with intramyocardial CSCs (26.9 ± 0.9%; $P < 0.01$; Fig. 8). In summary, CSC administration resulted in improvements in both LV remodeling (morphometry and echocardiography) and LV function (echocardiography and hemodynamic assessment). For some parameters, the improvement was significantly greater after intracoronary delivery than after intramyocardial injection of CSCs, suggesting that intracoronary infusion of CSCs in mice may be superior to intramyocardial delivery.

Survival and proliferation of transplanted CSCs

CSCs (obtained from GFP transgenic mice, passages 4–6) were transplanted into syngeneic C57BL/6 mouse hearts at 48 h after coronary reperfusion, either by intracoronary infusion or by intramyocardial injection. Mice were euthanized 39 days later. As shown in Fig. 9, the number of GFP^+ cells in both the risk region and the noninfarcted region was significantly greater after intracoronary than after intramyocardial injection. Evidence for differentiation of transplanted CSCs into new cardiac myocytes was provided by the presence of GFP^+ small cells that expressed α-sarcomeric actin, both in the intramyocardial injection group (Fig. 9c) and in the intracoronary infusion group (Fig. 9f). The appearance of these cells, however, was not that of mature cardiac myocytes (i.e., no sarcomeres were evident and cell size was small) (Fig. 9c, f). The total number of GFP/α-sarcomeric actin double positive cells in the risk region was significantly greater after intracoronary infusion than after intramyocardial delivery (Fig. 9g). The distribution of these cells was also different with the two administration modalities. In the intracoronary infusion group, most of the GFP/α-sarcomeric actin double positive cells were in the scar area rather than in the border zone (Fig. 9f, g). The opposite was observed in the intramyocardial injection group, in which most GFP/α-sarcomeric actin double positive cells were in the border zone (which was the site of needle injection) rather than in the scar (Fig. 9c, g).

To identify newly formed cells [32], BrdU was infused continuously for 39 days with mini-osmotic pumps beginning at the time of CSC transplantation and continuing until euthanasia. Evidence for formation of new myocytes was provided by the colocalization of α-sarcomeric actin and BrdU. As shown in Fig. 10, the incorporation of BrdU in the region at risk was significantly greater in CSC-treated hearts than in vehicle-treated hearts, both after intracoronary infusion and after intramyocardial injection. The total content of newly formed small cardiac myocytes (α-sarcomeric actin/BrdU double positive cells) in the risk region was higher after intracoronary infusion than after intramyocardial injection (29.9 ± 3.7% of all nuclei vs. 20.8 ± 4.0%, Fig. 10i), demonstrating that intracoronary administration of CSCs is associated with an overall increase in cellular proliferative activity in the risk region in the first few weeks after MI, which is consistent with the smaller scar area, the increased differentiation of CSCs into myocytes, and the greater attenuation of LV remodeling and improvement of LV function compared with intramyocardial delivery.

Discussion

An animal model of intracoronary stem cell therapy that enables use of transgenesis and gene targeting would be a powerful tool but is still lacking. To address this gap, the present investigation utilized a murine model of reperfused MI and compared the effects of intracoronary and intramyocardial delivery of murine $lin^-/c\text{-}kit^+/GFP^+$ CSCs on post-MI LV remodeling (dilation) and systolic as well as diastolic dysfunction using three independent techniques (morphometry, echocardiography, and hemodynamic studies) and a variety of functional parameters, both load-dependent and load-independent.

Salient findings

The salient results can be summarized as follows:

1. $Lin^-/c\text{-}kit^+/GFP^+$ CSCs can be successfully isolated and expanded from GFP^{Tg} mouse hearts and cultured in stable conditions with high purity and no detectable changes in phenotype for up to ten passages.
2. These cells exhibit properties typically described for CSCs in other species: vigorous proliferation, ability to express markers specific of endothelial, smooth muscle, and myocytic lineages, and migration to SDF-1.
3. Despite the small size of the murine heart and a large recent MI, intracoronary delivery of CSCs is technically feasible, is associated with acceptable mortality, and results in significant alleviation of post-MI adverse remodeling and dysfunction, at least equivalent, if not superior, to that achieved with intramyocardial delivery.
4. Intracoronary delivery of CSCs enables cells to reach and be uniformly distributed throughout the entire left ventricle; compared with intramyocardial injection, intracoronary infusion was associated with a more homogeneous distribution of cells in the infarcted region (Fig. 5).
5. The amount of viable tissue (Fig. 8), the number of GFP^+/alpha-sarcomeric actin positive cells (Fig. 9), and the number of $BrdU^+$/alpha-sarcomeric actin positive cells (Fig. 10) in the infarcted region were significantly increased both after intramyocardial and after intracoronary CSC delivery; however, the increases were greater in the latter, suggesting that intracoronary infusion resulted in greater formation of new cardiomyocytes.
6. The anterior (infarcted) wall was thicker (Fig. 8) and exhibited improved regional function (Figs. 6 and 7) in both the intramyocardial and the intracoronary cell-treated groups; these salubrious effects did not differ between the two groups.
7. In both groups, the LV end-diastolic and end-systolic volumes (Fig. 6) and the LV expansion index (Fig. 8) (which quantifies both the degree of LV dilation and the degree of infarct wall thinning: LV expansion index = [LV cavity area/LV total area] × [non-infarcted region wall thickness/risk region wall thickness] [22]) were significantly reduced, whilst the LV EF and other parameters of LV systolic and diastolic function were improved (Figs. 6, 7); overall, the magnitude of these effects was similar in the two groups.

Collectively, these data demonstrate that, in the murine model of reperfused MI, intracoronary CSC infusion is at least as effective as intramyocardial injection in limiting LV remodeling and improving both regional and global LV function. The intracoronary route appears to be superior in terms of uniformity of cell distribution and cell engraftment in the risk region, which may account for the greater amount of viable tissue observed in this

region; nevertheless, with the model and samples sizes used herein, these advantages were not sufficient to produce statistically significant differences in structural or functional outcome 39 days later.

Previous studies have delivered various types of stem cells in murine hearts by the intramyocardial or intravenous route [3, 31, 39]. However, to our knowledge, this is the first study to report that intracoronary infusion of stem cells in mice is feasible and effective. This is also the first study to use murine CSCs in a murine model of reperfused MI, which differs importantly from models of permanent coronary occlusion [3, 31, 39, 40].

Methodological considerations

The successful development of cell-based therapies for myocardial repair requires not only an efficient and clinically relevant method for cell delivery, but also an animal model that enables investigation of the molecular mechanisms that underlie the observed effects. The mouse is currently the best model to perform genetic manipulations that enable one to dissect the specific contribution of individual proteins. In previous studies in mice, cells were injected directly into the myocardium (usually in the peri-infarct region) [3, 31] or intravenously [39, 40], probably because these modes of delivery are technically easier than intracoronary infusion and, after intramyocardial injection, the short-term retention of the injected cells in the LV wall is higher. Our preliminary results show that intravenous injection of CSCs is ineffective (data not shown). Although these previous studies have documented the ability of various stem cells to alleviate LV remodeling and dysfunction [3, 31, 39, 40], intramyocardial injection of cells has significant inherent disadvantages. As shown in Fig. 5, when CSCs were injected directly into the border zone of the infarct with a needle, their distribution within the risk region 2 days later was patchy and highly inhomogeneous; predictably, the cells were clustered near the injection sites, whilst most of the infarct contained very few CSCs. Planimetric calculations indicate that only ~30–35% of the left ventricle contained any transplanted cells; thus, most of the left ventricle did not benefit directly from the procedure. In addition, intramyocardial injection would be difficult to use clinically on a widespread basis, for it would require invasive procedures that are not readily applicable in most hospitals and would be not only extremely cumbersome but also very expensive.

From a clinical standpoint, the most widely applicable technique for cell delivery is intracoronary infusion. Numerous clinical trials have used this modality, because it is simple, safe, and the most feasible in routine clinical practice. As indicated by recent meta-analyses [1], in the aggregate, clinical studies have shown that intracoronary infusion of cells resulted in enhanced global and regional LV function, reduction in infarct size, and improved clinical outcome, attesting to the therapeutic effectiveness of this approach and suggesting that intracoronary delivery is likely to remain a major (if not the major) mode of cell administration in patients. Consequently, the availability of a murine model of intracoronary cell therapy is important in order to conduct preclinical work in a clinically relevant manner. The fact that the mechanisms that underlie the encouraging clinical results remain unclear further underscores the importance of developing preclinical models that illuminate the molecular basis for the salubrious effects of intracoronary cell infusion.

Although salubrious effects of intracoronary infusion of stem cells have been reported in pigs [25] and rats [38], these models do not lend themselves well to molecular studies. While transgenesis or gene knockout are possible in larger mammals including pigs and rats [24, 33], developing such models would be extremely costly and time-consuming, and thus impractical. At present, the mouse is the only species in which the same gene can be manipulated by both transgenesis and gene knockout. Another advantageous feature of the murine model is the availability of GFP^{Tg} mice. Our results demonstrate that the use of

these mice enabled us to obtain a population of CSCs in which >99% of the cells expressed GFP, thereby facilitating the tracking of transplanted CSCs in vivo. In contrast, viral vector-mediated GFP gene transfer into CSCs, even when repeated thrice, results in only ~70% of cells expressing GFP [4]. All of these considerations emphasize the utility of a murine model of intracoronary cell infusion.

Thus far, almost all murine studies of stem cell therapy have used permanent coronary occlusions [3, 31, 39, 40]. One of the distinctive features of the model described herein is that MI was induced by a temporary coronary occlusion followed by reperfusion. The rationale is that in contemporary clinical practice, the majority of patients with acute MI undergo coronary reperfusion, either spontaneously or iatrogenically. Extrapolating concepts from the setting of a permanent to that of a temporary coronary occlusion is problematic because reperfusion dramatically changes the milieu of the infarcted tissue. For example, the inflammatory response and the generation of cytokines and reactive oxygen species (which have a major influence on stem cell function) are dramatically exaggerated after reperfusion. Consequently, a model of reperfused MI is more clinically relevant than a model of permanent coronary occlusion.

A 60-min duration of coronary occlusion was selected because it produces relatively large infarcts that average 60–70% of the risk region in control animals and result in LV remodeling and failure (Figs. 6, 7, 8). In pilot studies, shorter occlusions (30 or 45 min) did not consistently result in LV remodeling or failure (data not shown).

The rationale for using a fourfold higher number of cells with intracoronary (4×10^5) versus intramyocardial delivery (1×10^5) is that the efficiency of the i.c route is much less than that of the i.m. route. For example, the persistence of cells has been shown to be only 2.6 ± 0.3% after intracoronary infusion versus 11 ± 3% after intramyocardial injection [23]. Although intracoronary CSC infusion has the potential to produce microembolization, which may result in increased myocardial TNF-α and consequently cause contractile dysfunction [21, 26], we believe that this is unlikely because $lin^-/c\text{-}kit^+$ CSCs are small [the average diameter of the CSCs used in the current study was 8.08 ± 0.16 μm ($n = 96$) as measured by Image J (1.42q, NIH)].

Comparison of intramyocardial and intracoronary CSC delivery

In general, there were no major differences in outcome between intramyocardial and intracoronary delivery. With respect to regional LV structure and function, the effects of the two delivery routes were similar: despite a greater percent of viable tissue in the risk region after intracoronary infusion (Fig. 8), the improvement in diastolic wall thickness (measured by morphometry (Fig. 8) and echo-cardiography (Fig. 6) and in systolic wall thickening [measured by echocardiography (Fig. 6)] in the infarcted wall did not differ with the two approaches.

With regard to global LV structure and function, our results do not conclusively establish whether intracoronary infusion was superior to intramyocardial administration, because the differences between the two approaches were small and were not consistent between echocardiographic and hemodynamic studies. Echocardiographically, intra-coronary delivery resulted in a slightly but significantly greater improvement in LV end-diastolic volume, LV end-systolic volume, and LV EF compared with intramyocardial injection (Fig. 6); in contrast, hemodynamic analyses did not show any significant differences between the two delivery routes (Fig. 7). A thorough quantitative comparison would require dose–response studies. However, we feel that the doses of CSCs delivered with both routes were maximal or near-maximal, since in the small murine heart intramyocardial injection of >50 μl or intracoronary infusion of >100 μl would be difficult or even lethal.

Conclusions

We have described a murine model of intracoronary CSC infusion after a reperfused MI that should be useful in future investigations aimed at unraveling the molecular/cellular mechanisms responsible for the beneficial actions of this therapy. To our knowledge, this is the first report to demonstrate that intracoronary administration of stem cells in mice post-MI is feasible. This murine model of stem cell transplantation via intracoronary delivery should be useful for investigating the impact of genetic manipulations on physiological end-points after cell-based therapy in vivo. By applying this model to mice with overexpression or targeted disruption of individual genes implicated in the cellular pathways underlying the mechanism of cell-based therapy, it should be possible to conclusively establish the role of a specific gene product in the effects of stem cell therapy on cardiac structure and function in the intact animal. The clinical relevance of a murine model of intracoronary CSC delivery is underscored by the fact that CSCs are already being tested in a phase 1 clinical trial (SCIPIO [http://www.clinicaltrials.gov/ct2/show/NCT00474461]) with encouraging initial results [6], and that they can be reliably expanded from small endomyocardial biopsies for subsequent autologous administration [2, 10, 35].

Acknowledgments

This study was supported in part by NIH grants R01 HL55757, HL-70897, HL-76794, and P01HL78825.

References

1. Abdel-Latif A, Bolli R, Tleyjeh IM, Montori VM, Perin EC, Hornung CA, Zuba-Surma EK, Al-Mallah M, Dawn B. Adult bone marrow-derived cells for cardiac repair: a systematic review and meta-analysis. Arch Intern Med. 2007; 167:989–997.10.1001/archinte.167.10.989 [PubMed: 17533201]
2. Anversa P, Kajstura J, Leri A. If I can stop one heart from breaking. Circulation. 2007; 115:829–832.10.1161/CIRCULATIONAHA.106.682195 [PubMed: 17309932]
3. Bearzi C, Rota M, Hosoda T, Tillmanns J, Nascimbene A, De Angelis A, Yasuzawa-Amano S, Trofimova I, Siggins RW, Lecapitaine N, Cascapera S, Beltrami AP, D'Alessandro DA, Zias E, Quaini F, Urbanek K, Michler RE, Bolli R, Kajstura J, Leri A, Anversa P. Human cardiac stem cells. Proc Natl Acad Sci USA. 2007; 104:14068–14073.10.1073/pnas.0706760104 [PubMed: 17709737]
4. Beltrami AP, Barlucchi L, Torella D, Baker M, Limana F, Chimenti S, Kasahara H, Rota M, Musso E, Urbanek K, Leri A, Kajstura J, Nadal-Ginard B, Anversa P. Adult cardiac stem cells are multipotent and support myocardial regeneration. Cell. 2003; 114:763–776. [PubMed: 14505575]
5. Black RG Jr, Guo Y, Ge ZD, Murphree SS, Prabhu SD, Jones WK, Bolli R, Auchampach JA. Gene dosage-dependent effects of cardiac-specific overexpression of the A3 adenosine receptor. Circ Res. 2002; 91:165–172. [PubMed: 12142350]
6. Bolli R, Chugh AR, D'Amario D, Stoddard MF, Ikram S, Wagner SG, Beache GM, Leri A, Hosoda T, Loughran JH, Goihberg P, Fiorini C, Solankhi NK, Fahsah I, Chatterjee A, Elmore JB, Rokosh DG, Slaughter MS, Kajstura J, Anversa P. Use of cardiac stem cells for the treatment of heart failure: translation from bench to the clinical setting. Circ Res. 2010; 107:e32–e40.10.1161/RES.0b013e3182014899
7. Bolli R, Dawn B. The cornucopia of "pleiotropic" actions of statins: myogenesis as a new mechanism for statin-induced benefits? Circ Res. 2009; 104:144–146.10.1161/CIRCRESAHA.108.192500 [PubMed: 19179666]
8. Bolli R, Manchikalapudi S, Tang XL, Takano H, Qiu Y, Guo Y, Zhang Q, Jadoon AK. The protective effect of late preconditioning against myocardial stunning in conscious rabbits is mediated by nitric oxide synthase. Evidence that nitric oxide acts both as a trigger and as a mediator of the late phase of ischemic preconditioning. Circ Res. 1997; 81:1094–1107. [PubMed: 9400391]

9. Boni A, Urbanek K, Nascimbene A, Hosoda T, Zheng H, Delucchi F, Amano K, Gonzalez A, Vitale S, Ojaimi C, Rizzi R, Bolli R, Yutzey KE, Rota M, Kajstura J, Anversa P, Leri A. Notch1 regulates the fate of cardiac progenitor cells. Proc Natl Acad Sci USA. 2008; 105:15529–15534.10.1073/pnas.0808357105 [PubMed: 18832173]
10. D'Amario D, Fiorini C, Campbell PM, Goichberg P, Sanada F, Zheng H, Hosoda T, Rota M, Connell JM, Gallegos RP, Welt FG, Givertz MM, Mitchell RN, Leri A, Kajstura J, Pfeffer MA, Anversa P. Functionally Competent Cardiac Stem Cells Can Be Isolated From Endomyocardial Biopsies of Patients With Advanced Cardiomyopathies. Circ Res. 201110.1161/CIRCRESAHA.111.241380
11. Dawn B, Bolli R. Adult bone marrow-derived cells: regenerative potential, plasticity, and tissue commitment. Basic Res Cardiol. 2005; 100:494–503.10.1007/s00395-005-0552-5 [PubMed: 16237509]
12. Dawn B, Bolli R. Bone marrow for cardiac repair: the importance of characterizing the phenotype and function of injected cells. Eur Heart J. 2007; 28:651–652.10.1093/eurheartj/ehm009 [PubMed: 17339263]
13. Dawn B, Bolli R. Increasing evidence that estrogen is an important modulator of bone marrow-mediated cardiac repair after acute infarction. Circulation. 2006; 114:2203–2205.10.1161/CIRCULATIONAHA.106.658260 [PubMed: 17116779]
14. Dawn B, Guo Y, Rezazadeh A, Huang Y, Stein AB, Hunt G, Tiwari S, Varma J, Gu Y, Prabhu SD, Kajstura J, Anversa P, Ildstad ST, Bolli R. Postinfarct cytokine therapy regenerates cardiac tissue and improves left ventricular function. Circ Res. 2006; 98:1098–1105.10.1161/01.RES.0000218454.76784.66 [PubMed: 16556872]
15. Dawn B, Stein AB, Urbanek K, Rota M, Whang B, Rastaldo R, Torella D, Tang XL, Rezazadeh A, Kajstura J, Leri A, Hunt G, Varma J, Prabhu SD, Anversa P, Bolli R. Cardiac stem cells delivered intravascularly traverse the vessel barrier, regenerate infarcted myocardium, and improve cardiac function. Proc Natl Acad Sci USA. 2005; 102:3766–3771.10.1073/pnas.0405957102 [PubMed: 15734798]
16. Dawn B, Tiwari S, Kucia MJ, Zuba-Surma EK, Guo Y, Sanganalmath SK, Abdel-Latif A, Hunt G, Vincent RJ, Taher H, Reed NJ, Ratajczak MZ, Bolli R. Transplantation of bone marrow-derived very small embryonic-like stem cells attenuates left ventricular dysfunction and remodeling after myocardial infarction. Stem Cells. 2008; 26:1646–1655.10.1634/stemcells.2007-0715 [PubMed: 18420834]
17. Feldman MD, Erikson JM, Mao Y, Korcarz CE, Lang RM, Freeman GL. Validation of a mouse conductance system to determine LV volume: comparison to echocardiography and crystals. Am J Physiol Heart Circ Physiol. 2000; 279:H1698–H1707. [PubMed: 11009457]
18. Georgakopoulos D, Mitzner WA, Chen CH, Byrne BJ, Millar HD, Hare JM, Kass DA. In vivo murine left ventricular pressure–volume relations by miniaturized conductance micromanometry. Am J Physiol. 1998; 274:H1416–H1422. [PubMed: 9575947]
19. Guo Y, Jones WK, Xuan YT, Tang XL, Bao W, Wu WJ, Han H, Laubach VE, Ping P, Yang Z, Qiu Y, Bolli R. The late phase of ischemic preconditioning is abrogated by targeted disruption of the inducible NO synthase gene. Proc Natl Acad Sci USA. 1999; 96:11507–11512. [PubMed: 10500207]
20. Halkos ME, Zhao ZQ, Kerendi F, Wang NP, Jiang R, Schmarkey LS, Martin BJ, Quyyumi AA, Few WL, Kin H, Guyton RA, Vinten-Johansen J. Intravenous infusion of mesenchymal stem cells enhances regional perfusion and improves ventricular function in a porcine model of myocardial infarction. Basic Res Cardiol. 2008; 103:525–536.10.1007/s00395-008-0741-0 [PubMed: 18704259]
21. Heusch G, Kleinbongard P, Bose D, Levkau B, Haude M, Schulz R, Erbel R. Coronary microembolization: from bedside to bench and back to bedside. Circulation. 2009; 120:1822–1836.10.1161/CIRCULATIONAHA.109.888784 [PubMed: 19884481]
22. Hochman JS, Choo H. Limitation of myocardial infarct expansion by reperfusion independent of myocardial salvage. Circulation. 1987; 75:299–306. [PubMed: 3791612]
23. Hou D, Youssef EA, Brinton TJ, Zhang P, Rogers P, Price ET, Yeung AC, Johnstone BH, Yock PG, March KL. Radio-labeled cell distribution after intramyocardial, intracoronary, and interstitial

retrograde coronary venous delivery: implications for current clinical trials. Circulation. 2005; 112:I150–I156.10.1161/CIRCULATIONAHA.104.526749 [PubMed: 16159808]

24. Jakobsen JE, Li J, Kragh PM, Moldt B, Lin L, Liu Y, Schmidt M, Winther KD, Schyth BD, Holm IE, Vajta G, Bolund L, Callesen H, Jorgensen AL, Nielsen AL, Mikkelsen JG. Pig transgenesis by Sleeping Beauty DNA transposition. Transgenic Res. 201010.1007/s11248-010-9438-x
25. Johnston PV, Sasano T, Mills K, Evers R, Lee ST, Smith RR, Lardo AC, Lai S, Steenbergen C, Gerstenblith G, Lange R, Marban E. Engraftment, differentiation, and functional benefits of autologous cardiosphere-derived cells in porcine ischemic cardiomyopathy. Circulation. 2009; 120:1075–1083. 1077 p following 1083. 10.1161/CIRCULATIONAHA.108.816058 [PubMed: 19738142]
26. Kleinbongard P, Heusch G, Schulz R. TNFalpha in atherosclerosis, myocardial ischemia/reperfusion and heart failure. Pharmacol Ther. 2010; 127:295–314.10.1016/j.pharmthera.2010.05.002 [PubMed: 20621692]
27. Li Q, Guo Y, Ou Q, Cui C, Wu WJ, Tan W, Zhu X, Lanceta LB, Sanganalmath SK, Dawn B, Shinmura K, Rokosh GD, Wang S, Bolli R. Gene transfer of inducible nitric oxide synthase affords cardioprotection by upregulating heme oxygenase-1 via a nuclear factor-{kappa}B-dependent pathway. Circulation. 2009; 120:1222–1230.10.1161/CIRCULATIONAHA.108.778688 [PubMed: 19752329]
28. Li Q, Guo Y, Tan W, Ou Q, Wu WJ, Sturza D, Dawn B, Hunt G, Cui C, Bolli R. Cardioprotection afforded by inducible nitric oxide synthase gene therapy is mediated by cyclooxygenase-2 via a nuclear factor-kappaB dependent pathway. Circulation. 2007; 116:1577–1584.10.1161/CIRCULATIONAHA.107.689810 [PubMed: 17785622]
29. Li Q, Guo Y, Tan W, Stein AB, Dawn B, Wu WJ, Zhu X, Lu X, Xu X, Siddiqui T, Tiwari S, Bolli R. Gene therapy with iNOS provides long-term protection against myocardial infarction without adverse functional consequences. Am J Physiol Heart Circ Physiol. 2006; 290:H584–H589.10.1152/ajpheart.00855.2005 [PubMed: 16172153]
30. Li Q, Guo Y, Xuan YT, Lowenstein CJ, Stevenson SC, Prabhu SD, Wu WJ, Zhu Y, Bolli R. Gene therapy with inducible nitric oxide synthase protects against myocardial infarction via a cyclooxygenase-2-dependent mechanism. Circ Res. 2003; 92:741–748. [PubMed: 12702642]
31. Orlic D, Kajstura J, Chimenti S, Jakoniuk I, Anderson SM, Li B, Pickel J, McKay R, Nadal-Ginard B, Bodine DM, Leri A, Anversa P. Bone marrow cells regenerate infarcted myocardium. Nature. 2001; 410:701–705.10.1038/3507058735070587 [PubMed: 11287958]
32. Padin-Iruegas ME, Misao Y, Davis ME, Segers VF, Esposito G, Tokunou T, Urbanek K, Hosoda T, Rota M, Anversa P, Leri A, Lee RT, Kajstura J. Cardiac progenitor cells and biotinylated insulin-like growth factor-1 nanofibers improve endogenous and exogenous myocardial regeneration after infarction. Circulation. 2009; 120:876–887.10.1161/CIRCULATIONAHA.109.852285 [PubMed: 19704095]
33. Pravenec M, Zidek V, Landa V, Simakova M, Mlejnek P, Silhavy J, Maxova M, Kazdova L, Seidman JG, Seidman CE, Eminaga S, Gorham J, Wang J, Kurtz TW. Age-related autocrine diabetogenic effects of transgenic resistin in spontaneously hypertensive rats: gene expression profile analysis. Physiol Genomics. 201110.1152/physiolgenomics.00112.2010
34. Ridley AJ, Schwartz MA, Burridge K, Firtel RA, Ginsberg MH, Borisy G, Parsons JT, Horwitz AR. Cell migration: integrating signals from front to back. Science. 2003; 302:1704–1709.10.1126/science.1092053302/5651/1704 [PubMed: 14657486]
35. Rota M, Padin-Iruegas ME, Misao Y, De Angelis A, Maestroni S, Ferreira-Martins J, Fiumana E, Rastaldo R, Arcarese ML, Mitchell TS, Boni A, Bolli R, Urbanek K, Hosoda T, Anversa P, Leri A, Kajstura J. Local activation or implantation of cardiac progenitor cells rescues scarred infarcted myocardium improving cardiac function. Circ Res. 2008; 103:107–116.10.1161/CIRCRESAHA.108.178525 [PubMed: 18556576]
36. Schuh A, Liehn EA, Sasse A, Schneider R, Neuss S, Weber C, Kelm M, Merx MW. Improved left ventricular function after transplantation of microspheres and fibroblasts in a rat model of myocardial infarction. Basic Res Cardiol. 2009; 104:403–411.10.1007/s00395-008-0763-7 [PubMed: 19139948]

37. Stein AB, Tiwari S, Thomas P, Hunt G, Levent C, Stoddard MF, Tang XL, Bolli R, Dawn B. Effects of anesthesia on echocardiographic assessment of left ventricular structure and function in rats. Basic Res Cardiol. 2007; 102:28–41.10.1007/s00395-006-0627-y [PubMed: 17006633]

38. Tang XL, Rokosh G, Sanganalmath SK, Yuan F, Sato H, Mu J, Dai S, Li C, Chen N, Peng Y, Dawn B, Hunt G, Leri A, Kajstura J, Tiwari S, Shirk G, Anversa P, Bolli R. Intracoronary administration of cardiac progenitor cells alleviates left ventricular dysfunction in rats with a 30-day-old infarction. Circulation. 2010; 121:293–305.10.1161/CIRCULATIONAHA.109.871905 [PubMed: 20048209]

39. Tang YL, Zhu W, Cheng M, Chen L, Zhang J, Sun T, Kishore R, Phillips MI, Losordo DW, Qin G. Hypoxic preconditioning enhances the benefit of cardiac progenitor cell therapy for treatment of myocardial infarction by inducing CXCR4 expression. Circ Res. 2009; 104:1209–1216.10.1161/CIRCRESAHA.109.197723 [PubMed: 19407239]

40. Tseng A, Stabila J, McGonnigal B, Yano N, Yang MJ, Tseng YT, Davol PA, Lum LG, Padbury JF, Zhao TC. Effect of disruption of Akt-1 of lin(-)c-kit(+) stem cells on myocardial performance in infarcted heart. Cardiovasc Res. 2010; 87:704–712.10.1093/cvr/cvq110 [PubMed: 20410290]

41. Urbanek K, Cesselli D, Rota M, Nascimbene A, De Angelis A, Hosoda T, Bearzi C, Boni A, Bolli R, Kajstura J, Anversa P, Leri A. Stem cell niches in the adult mouse heart. Proc Natl Acad Sci USA. 2006; 103:9226–9231.10.1073/pnas.0600635103 [PubMed: 16754876]

42. Yang B, Larson DF, Watson R. Age-related left ventricular function in the mouse: analysis based on in vivo pressure-volume relationships. Am J Physiol. 1999; 277:H1906–H1913. [PubMed: 10564146]

43. Zuba-Surma EK, Guo Y, Taher H, Sanganalmath SK, Hunt G, Vincent RJ, Kucia M, Abdel-Latif A, Tang XL, Ratajczak MZ, Dawn B, Bolli R. Transplantation of expanded bone marrow-derived very small embryonic-like stem cells (VSEL-SCs) improves left ventricular function and remodeling after myocardial infarction. J Cell Mol Med. 201010.1111/j.1582-4934.2010.01126.x

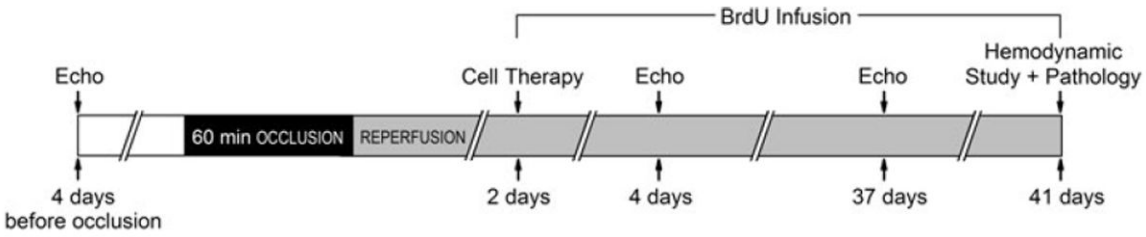

Fig. 1.

Experimental protocol. Mice were subjected a 60-min coronary occlusion followed by 41 days of reperfusion. CSCs or vehicle were delivered at 48 h after reperfusion. Serial echocardiographic studies were performed at baseline (4 days prior to coronary occlusion), 2 days after CSC transplantation (4 days after reperfusion), and 35 days after CSC transplantation (37 days after reperfusion, and 4 days prior to euthanasia). To assess CSC proliferation, mice were given BrdU (33 mg/kg/day, using mini-osmotic pumps) throughout the 39-day follow-up period after CSC transplantation. At 39 days after CSC transplantation (41 days after reperfusion), mice underwent a hemodynamic study and were euthanized, after which the hearts were harvested for morphometric and histopathologic analyses

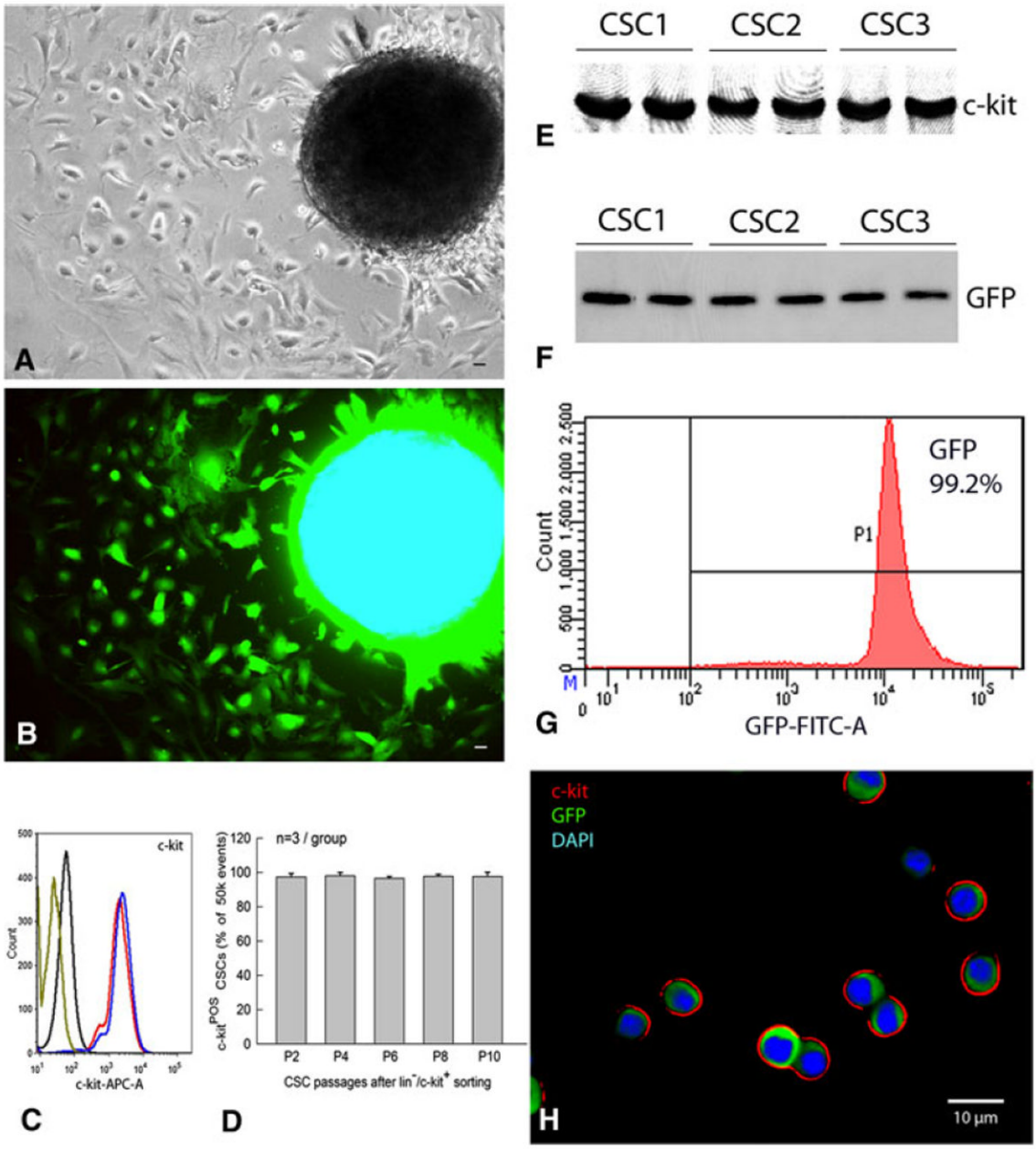

Fig. 2.

Isolation and characterization of murine CSCs. At 7 days after primary culture of a fragment of atrial myocardium obtained from a GFP^{Tg} mouse heart, GFP^{+} cells grew around the periphery of the spherical tissue aggregate (**a**, phase contrast; **b**, epifluorescence). **c** Profile of the sorted $lin^{-}/c\text{-}kit^{+}$ CSCs (passage 4) labeled with anti-c-kit antibody (*red* and *blue*, duplicate assays), labeled with secondary antibody only (*black*), or unstained (*olive*). FACS analysis shows that c-kit expression is very high (>95%) and is stable for up to ten passages in cultured CSCs (**d**), which is consistent with the results of the Western blotting analysis of three independent CSC protein samples (passage 6) (**e**). **f** The same three independent CSC protein samples (passage 6) show GFP expression by Western blotting analysis, indicating that these cells are $c\text{-}kit^{+}/GFP^{+}$. **g** FACS analysis demonstrates robust GFP expression in

>99% of the sorted $lin^-/c\text{-}kit^+/GFP^+$ CSCs (passage 5). **h** smears of the sorted $lin^-/c\text{-}kit^+/GFP^+$ CSCs expressing c-kit (*red*) and GFP (*green*). Nuclei are stained with DAPI (*blue*). *Bars* 10 μm

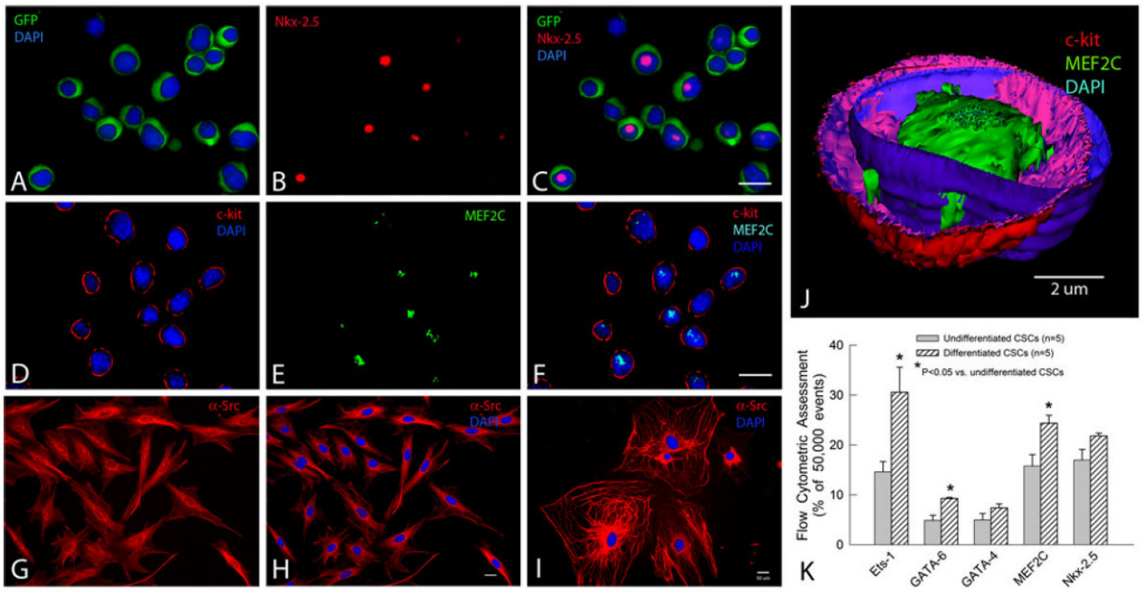

Fig. 3.

Profile and differentiation of murine CSCs. **a–c** Lin^{-}/c-kit^{+}/GFP^{+} CSCs cultured in growth medium at passage 4 express GFP in the cytoplasm (*green*) and, in some cases, the early cardiac transcription factor Nkx-2.5 in the nucleus (*red*). **d–f**: Lin^{-}/c-kit^{+}/GFP^{+} CSCs cultured in growth medium at passage 2 express c-kit on the membrane (*red*) and, in some cases, the early cardiac transcription factor MEF2C in the nucleus (*green*). CSCs cultured in differentiation medium in Matrigel for 10 days (**g–h**) or in the culture plate without Matrigel for 50 days (**i**) express the cardiac marker α-sarcomeric actin in the cytoplasm (*red*) (**g–i**) and display a cardiac myocyte-like morphology (**i**). **j** A 3-D computer reconstruction based on 42 confocal microscopic images showing a CSC that expresses c-kit (*red*) on the membrane and the early cardiac transcription factor MEF2C (*green*) in the nucleus. The nuclear membrane is stained with DAPI (*blue*). **k** FACS analysis of CSCs cultured for 10 days in differentiation medium shows increased expression of the lineage markers Ets-1 (endothelial), GATA-6 (smooth muscle), and GATA-4, MEF2C, and Nkx-2.5 (cardiac), demonstrating that lin^{-}/c-kit^{+}/GFP^{+} CSCs are heterogeneous and possess the potential to commit to all three components of the cardiac lineage. Data are mean ± SEM. *Bars* 10 μm

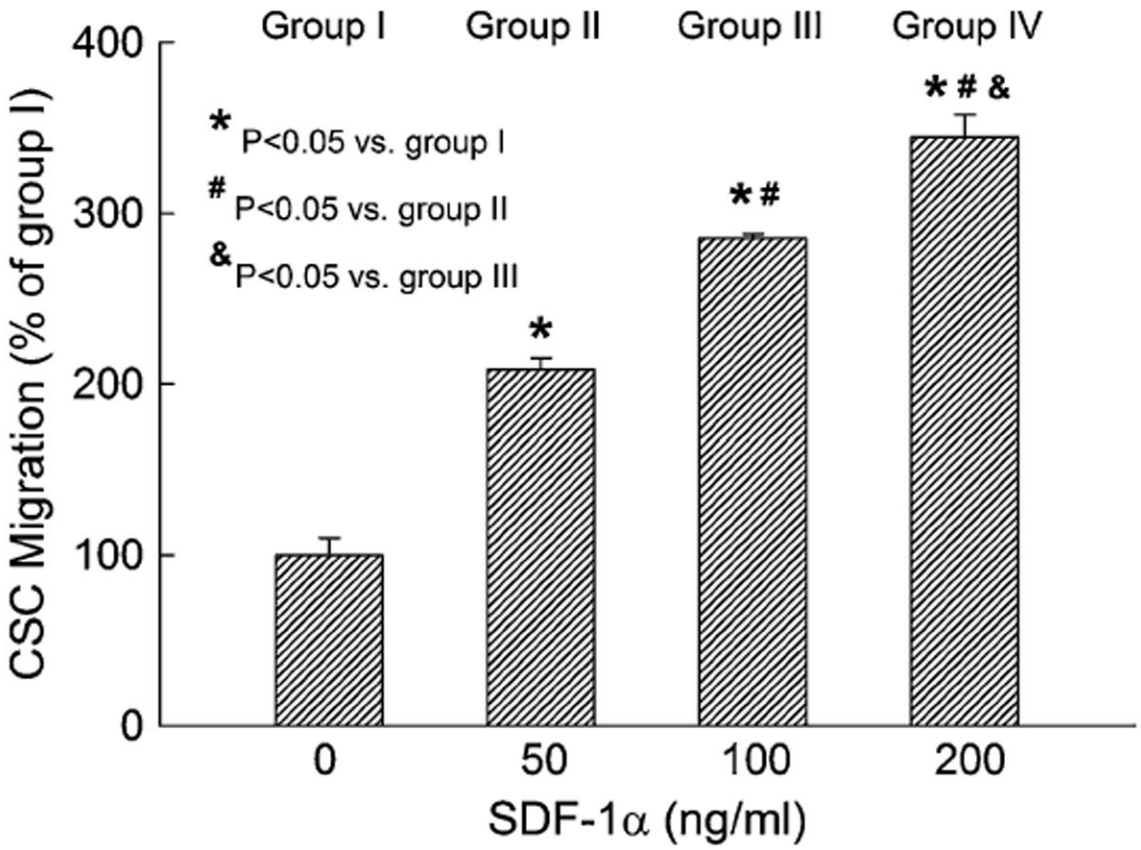

Fig. 4.

Murine CSC migration toward increasing concentrations of SDF-1α. Migration was determined with the Boyden chamber assay. Shown are results obtained from four independent experiments performed in duplicate. Data are mean ± SEM. *n* = 4/group

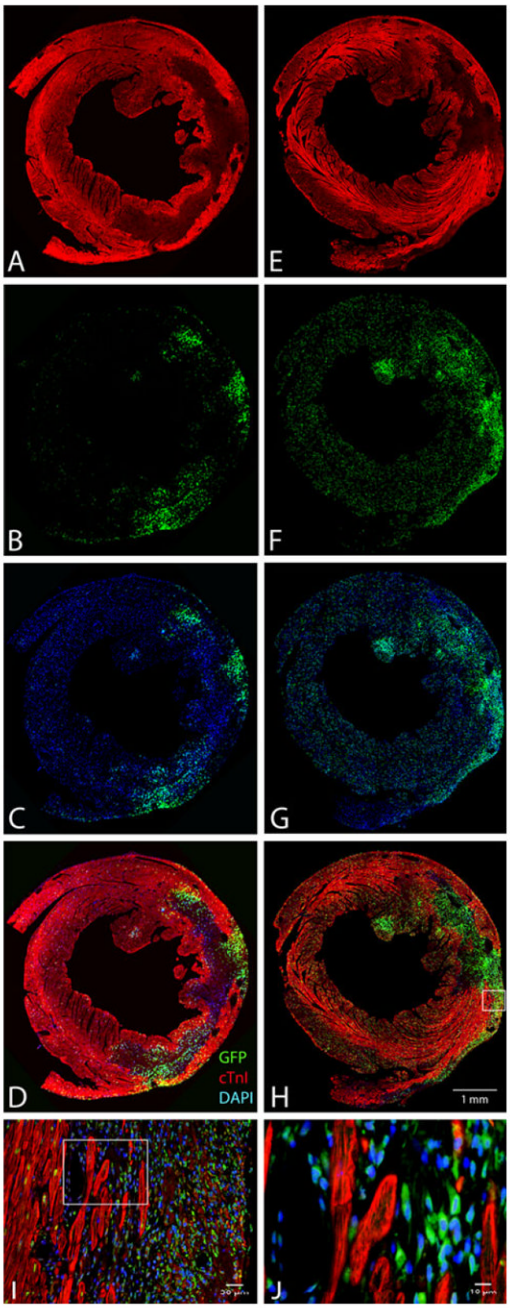

Fig. 5.

Distribution of GFP$^+$ CSCs in the heart following transplantation. Six mice underwent a 60-min coronary occlusion followed by reperfusion; CSCs were transplanted 48 h after reperfusion either via intramyocardial injection (**a–d**) or via intracoronary infusion (**e–h**). Shown are representative microscopic images of LV sections obtained 2 days after CSC transplantation (i.e., 4 days after reperfusion). Immunofluorescent staining is illustrated for GFP (*green*), troponin I (*red*), and DAPI (*blue*). **i** is a higher magnification image of the box in **h**, and **j** is a higher magnification image of the box in **i**. These analyses were repeated in three mice that received intramyocardial injection and in three mice that received intracoronary injection

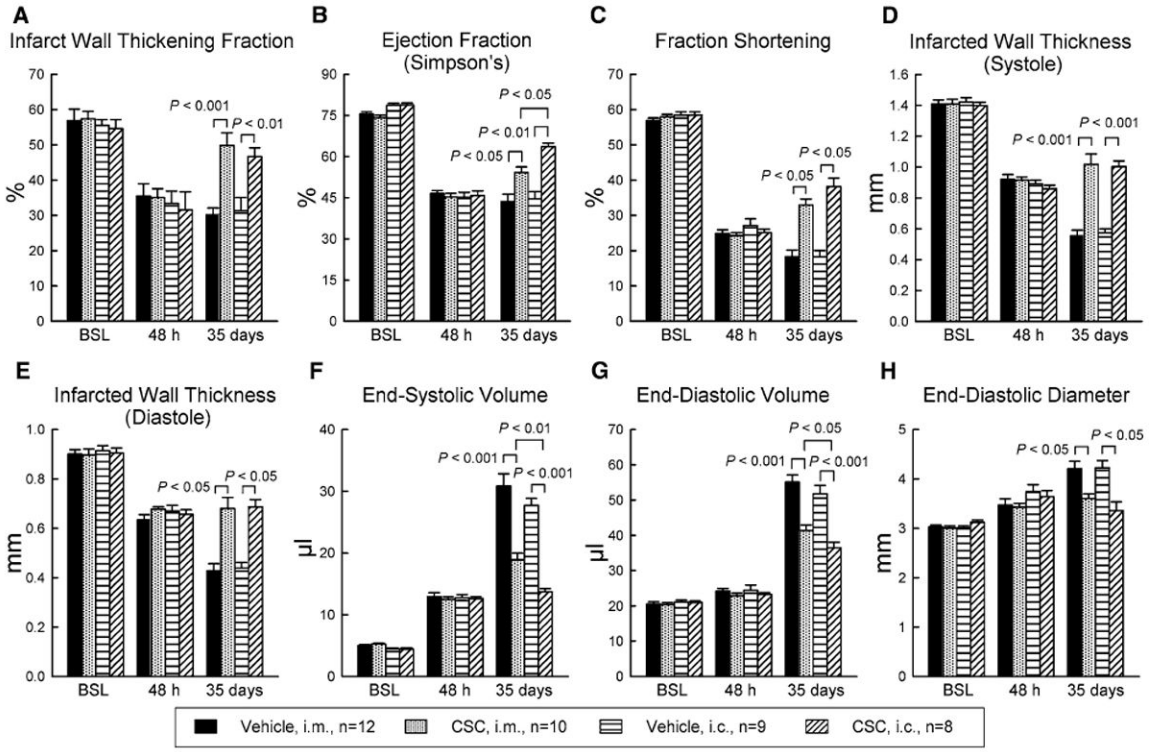

Fig. 6.

Effect of transplantation of CSCs on LV function. Serial echocardiographic studies were performed at baseline (BSL, 4 days prior to coronary occlusion/reperfusion), 48 h after CSC treatment (4 days after reperfusion), and 35 days after CSC transplantation (37 days after reperfusion and 4 days prior to euthanasia). i.m., intramyocardial injection; i.c., intracoronary infusion. Data are mean ± SEM

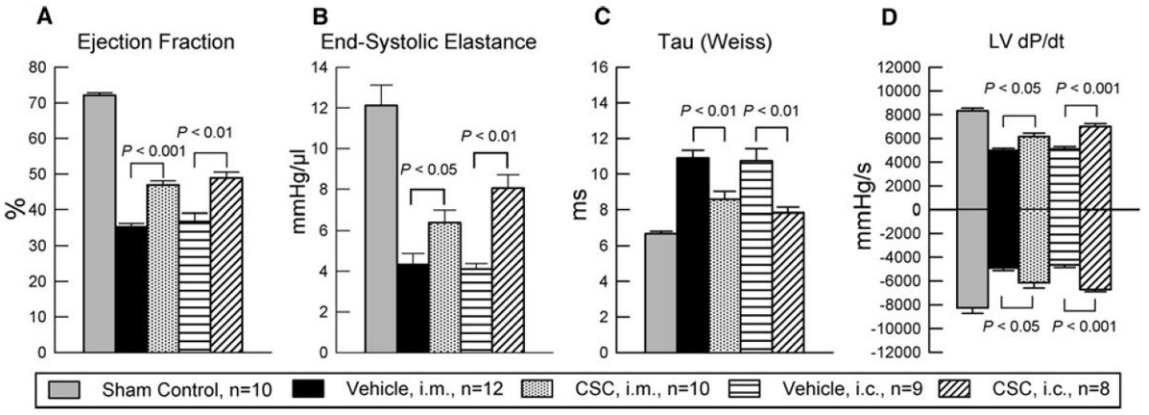

Fig. 7.

Hemodynamic assessment of LV function at 39 days after intracoronary infusion (i.c.) or intramyocardial injection (i.m.) of CSCs and in age-matched mice not subjected to surgery (sham control group). The figure shows LV ejection fraction, end-systolic elastance, Tau (Weiss), and LV dP/dt. Data are mean ± SEM

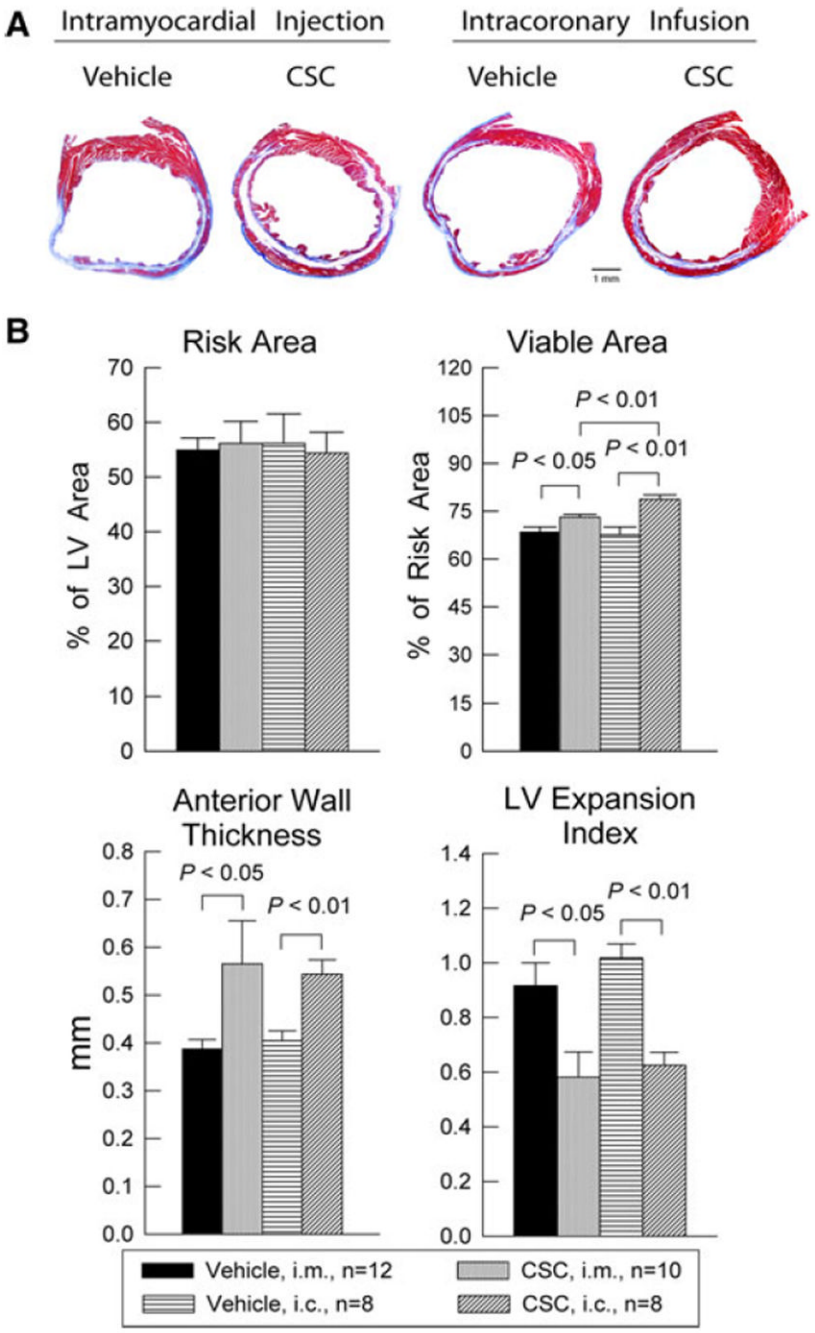

Fig. 8.

Morphometric analysis of LV remodeling after CSC transplantation. **a** Representative Masson's trichrome-stained myocardial sections from the intramyocardial injection groups (i.m.) treated with vehicle or CSCs, and from the intracoronary infusion groups (i.c.) treated with vehicle or CSCs. Scar tissue and viable myocardium are identified in *blue* and *red*, respectively. **b** quantitative analysis of LV morphometric parameters. *LV* left ventricle; LV expansion index = (LV cavity area/LV total area) × (non-infarcted region wall thickness/risk region wall thickness). Data are mean ± SEM

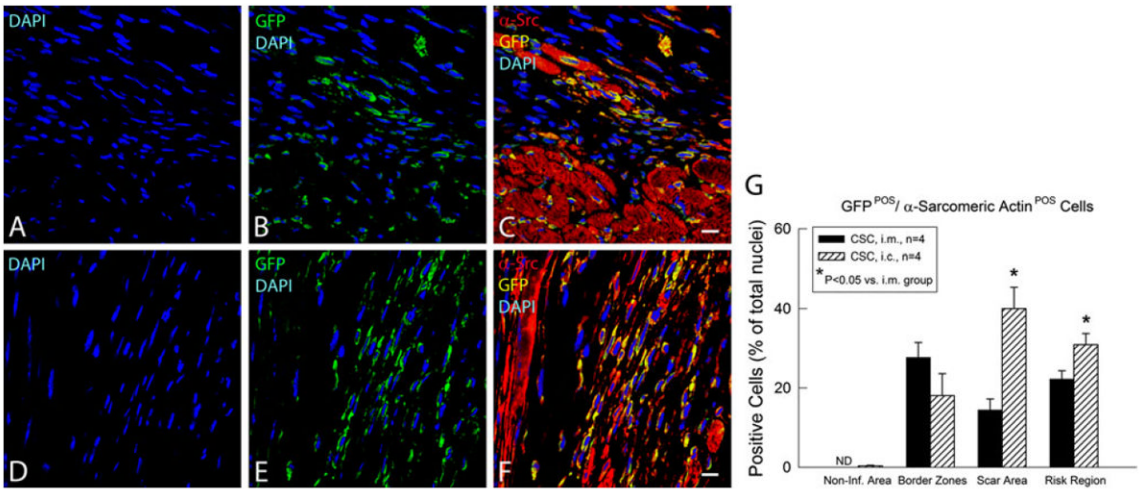

Fig. 9.

Fate of transplanted CSCs 39 days after intramyocardial injection (i.m.) or intracoronary infusion (i.c.). Survival and differentiation of transplanted CSCs were determined by immunofluorescent detection of GFP (*green*), α-sarcomeric actin (*red*), GFP/α-sarcomeric actin double positivity (*yellow*), and nuclear DAPI (*blue*) in hearts that received CSCs either by the i.m. (**a–c**) or by the i.c (**d–f**) route. Shown are representative confocal microscopic images obtained from the infarcted area 39 days after CSC transplantation. **g** Quantitative analysis of the number of GFP/α-sarcomeric actin double positive cells. Data are mean ± SEM. *ND* Non-Detectable. The region at risk comprises both the border zones and the scar area. *Bars* 10 μm

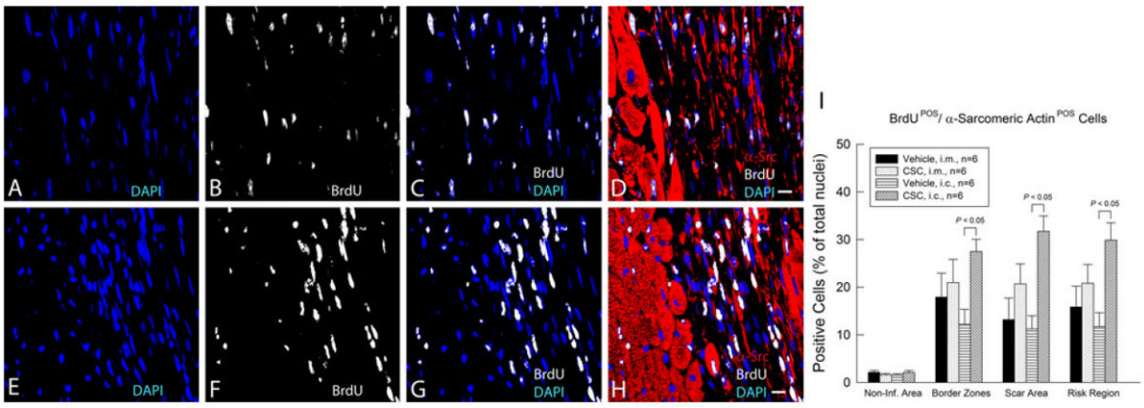

Fig. 10.

Proliferation of transplanted CSCs over the 39-day period after intramyocardial injection (i.m.) or intracoronary infusion (i.c.). CSCs were given 48 h after reperfusion by the i.m. or the i.c. route; mice received BrdU beginning at the time of cell transplantation and continuing until euthanasia (for 39 days). Positivity for BrdU (*white*) in representative confocal microscopic images obtained from the infarcted area identifies newly formed cells (**a–d**, i.m. group; **e–h**, i.c. group). α-Sarcomeric actin is red. Nuclei are stained with DAPI (*blue*). **i** Quantitative analysis of the number of BrdU/α-sarcomeric actin double positive cells (newly formed cells with apparent commitment to myocytic differentiation) at 39 days after CSC transplantation. Data are mean ± SEM. The region at risk comprises both the border zones and the scar area. *Bars* 10 μm

Table 1

Heart rate and body temperature during echocardiographic and hemodynamic studies

	Echo	Echo		Hemodynamic Study
	BSL	4 days	37 days	41 days
Heart rate (beats/min)				
Vehicle, i.m., $n = 12$	469 ± 10	497 ± 19	481 ± 10	458 ± 7
CSC, i.m., $n = 10$	448 ± 9	461 ± 10	481 ± 15	455 ± 12
Vehicle, i.c., $n = 9$	523 ± 10[a, b]	596 ± 21[a, b]	513 ± 13	471 ± 15
CSC, i.c., $n = 8$	521 ± 7[a, b]	567 ± 11[a, b]	555 ± 24[a, b]	490 ± 8
Temperature (°C)				
Vehicle, i.m., $n = 12$	37.2 ± 0.0	37.2 ± 0.1	37.3 ± 0.1	37.0 ± 0.0
CSC, i.m., $n = 10$	37.1 ± 0.1	37.1 ± 0.2	37.2 ± 0.0	37.1 ± 0 1
Vehicle i.c., $n = 9$	37.0 ± 0.1	37.0 ± 0.1	37.2 ± 0.1	37.0 ± 0.0
CSC, i.c., $n = 8$	37.2 ± 0.1	36.9 ± 0.1	37.2 ± 0.1	37.2 ± 0.1

Data are mean ± SEM. The heart rale and rectal temperature were recorded 4 days prior to coronary occlusion (BSL, baseline), 4 days, 37 days and 41 days after reperfusion. Rectal temperature was continuously monitored and carefully controlled throughout the experiment, as detailed in the text

[a] $P < 0.05$ versus Vehicle, i.m. group

[b] $P < 0.05$ versus CSC, i.m. group